

Effect of elastic boundary conditions on morphotropic $\text{Pb}(\text{Zr},\text{Ti})\text{O}_3$ piezoelectrics

A. Amin

Advanced Development Laboratory, Texas Instruments Inc., Attleboro, Massachusetts 02703

R. E. Newnham and L. E. Cross

Materials Research Laboratory, University Park, Pennsylvania 16802

(Received 13 February 1986)

Most of the technologically important transducers are made of poled-polycrystalline lead zirconate—lead titanate $\text{Pb}(\text{Zr},\text{Ti})\text{O}_3$ compositions near the morphotropic phase boundary where the $[\text{Zr}]:[\text{Ti}]$ ratio is approximately 1:1. The effect of elastic boundary conditions on single-domain stability and properties of compositions near the morphotropic phase boundary in the PbZrO_3 - PbTiO_3 phase diagram is of considerable interest, since in a polycrystalline ensemble, the elastic and electric boundary conditions are uncertain. In this work, a phenomenological free-energy function which we developed earlier is used to determine the influence of elastic boundary conditions upon the relative stability points and the rhombohedral ($R3m$)—tetragonal ($P4mm$) degeneracy required for the morphotropy at $[\text{Zr}]:[\text{Ti}]$ ratio near 1:1.

INTRODUCTION

The lead zirconate-titanate (PZT) crystalline solution between antiferroelectric lead zirconate (PbZrO_3) and ferroelectric lead titanate (PbTiO_3) contains a number of extremely important compositions used in the electronics industry. These compositions are grouped near the morphotropic phase boundary (MPB), where the $[\text{Zr}]:[\text{Ti}] \approx 1:1$ ratio (Fig. 1). Transducer elements such as sonar transmitters and detectors are made of poled PZT compositions near the MPB where the dielectric-constant, piezoelectric, and electromechanical coupling coefficients are unusually high.¹

The Landau-Ginzberg-Devonshire (LGD) phenomenological theory,^{2,3} for proper ferroelectrics has been suc-

cessfully applied to the PbZrO_3 - PbTiO_3 system.^{4,5} This free-energy function correctly predicts the relative stability points of the different phases in the solid-state portion of the PZT phase diagram. It also permits for the first time the calculation of the observed physical properties (e.g., dielectric, piezoelectric, and other coupling coefficients) as a function of temperature,⁴ electric field,⁶ and mechanical stress over the entire range of single-cell compositions.

FREE-ENERGY FUNCTION

Consider the free-energy density function for a proper ferroelectric derived from a prototypic phase of symmetry $Pm3m$. For Brillouin-zone-center modes, the free energy may be written as a power series^{2,3} in dielectric polarization P_i ($i = 1, 2, 3$) as follows:

$$\begin{aligned}
 G = & \alpha_1(P_1^2 + P_2^2 + P_3^2) + \alpha_{11}(P_1^4 + P_2^4 + P_3^4) + \alpha_{12}(P_1^2P_2^2 + P_2^2P_3^2 + P_3^2P_1^2) + \alpha_{111}(P_1^6 + P_2^6 + P_3^6) \\
 & + \alpha_{112}[P_1^4(P_2^2 + P_3^2) + P_2^4(P_3^2 + P_1^2) + P_3^4(P_1^2 + P_2^2)] + \alpha_{123}P_1^2P_2^2P_3^2 - \frac{1}{2}s_{11}(X_1^2 + X_2^2 + X_3^2) \\
 & - s_{12}(X_1X_2 + X_2X_3 + X_3X_1) - \frac{1}{2}s_{44}(X_4^2 + X_5^2 + X_6^2) - Q_{11}(X_1P_1^2 + X_2P_2^2 + X_3P_3^2) \\
 & - Q_{12}[X_1(P_2^2 + P_3^2) + X_2(P_3^2 + P_1^2) + X_3(P_1^2 + P_2^2)] - Q_{44}(X_4P_2P_3 + X_5P_3P_1 + X_6P_1P_2), \quad (1)
 \end{aligned}$$

where $\alpha_i, \alpha_{ij}, \alpha_{ijk}$ (in reduced tensor notation) are the dielectric stiffness and high-order stiffness coefficients at constant stress, s_{11}, s_{12}, s_{44} are the elastic compliances measured at constant polarization, and Q_{11}, Q_{12}, Q_{44} are the electrostriction constants written in polarization notation. The reduced tensor notation is used to describe the stress tensor in the free-energy expression [Eq. (1)]. In this notation the tensile stresses X_{11}, X_{22}, X_{33} are denoted by X_1, X_2, X_3 , respectively, and the shear components

X_{12}, X_{13}, X_{23} by X_6, X_5, X_4 , respectively. The expression is complete up to all six power terms in polarization, but contains only first-order terms in electrostrictive and elastic behavior. All the tensor coefficients in the free-energy function [Eq. (1)] which fit the experimental PbZrO_3 - PbTiO_3 phase diagram and the observed physical properties under zero stresses [all X_i vanish in Eq. (1)] have been determined,⁴ and are given in Table I.

A valid general criticism of the application of the LGD

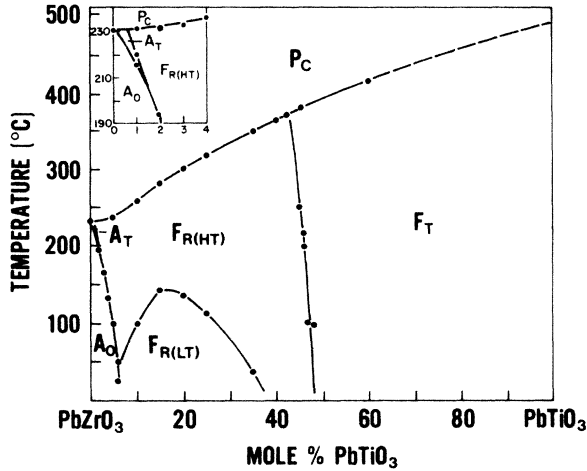


FIG. 1. Lead zirconate (PbZrO_3)—Lead titanate (PbTiO_3) phase diagram.

formalism to the description of the elastodielectric properties of a general nonlinear solid is that in using the simple infinitesimal strain formulation and the simple conventional definition of polarization the resulting electrostriction tensor coefficients are not strictly invariant under rotation of axes. The proper variables are the Lagrangian strain and the material measure of polarization or their proper thermodynamic conjugate variables;⁷ in this manner, the resulting internal energy function of the system is invariant under rigid rotations. However, it has been shown by Barsch *et al.*⁷ that for the special case of the simple proper ferroelectrics, in which the dielectric stiffness is anomalously small while the elastic compliance is almost normal, the correction terms to the simply formulated electrostriction constants are quite small.

In this work, the free-energy function [Eq. (1)] is used to calculate the influence of some postulated hydrostatic pressures upon the relative phase stabilities, and the rhombohedral ($R3m$)—tetragonal ($P4mm$) degeneracy required for the morphotropy at $[\text{Zr}]:[\text{Ti}] \approx 1:1$ ratio under zero stress.

INFLUENCE OF HYDROSTATIC PRESSURE

To assess the relative phase stabilities and the physical properties of morphotropic PZT compositions under a static stress system, it is necessary to consider various stress (X_i) levels and their effect on the free-energy function. For a hydrostatic pressure σ the following conditions apply.

$$X_1 = X_2 = X_3 = \sigma, \quad X_4 = X_5 = X_6 = 0.$$

Under these conditions the free-energy function [Eq. (1)] takes the form

$$G = -(3s_{11} + 6s_{12})\sigma^2/2 + [\alpha_1 + (Q_{11} + 2Q_{12})\sigma](P_1^2 + P_2^2 + P_3^2) + \alpha_{11}(P_1^4 + P_2^4 + P_3^4) + \alpha_{12}(P_1^2 P_2^2 + P_2^2 P_3^2 + P_3^2 P_1^2) + \alpha_{111}(P_1^6 + P_2^6 + P_3^6) + \alpha_{112}[P_1^4(P_2^2 + P_3^2) + P_2^4(P_3^2 + P_1^2) + P_3^4(P_1^2 + P_2^2)] + \alpha_{123}P_1^2 P_2^2 P_3^2. \quad (2)$$

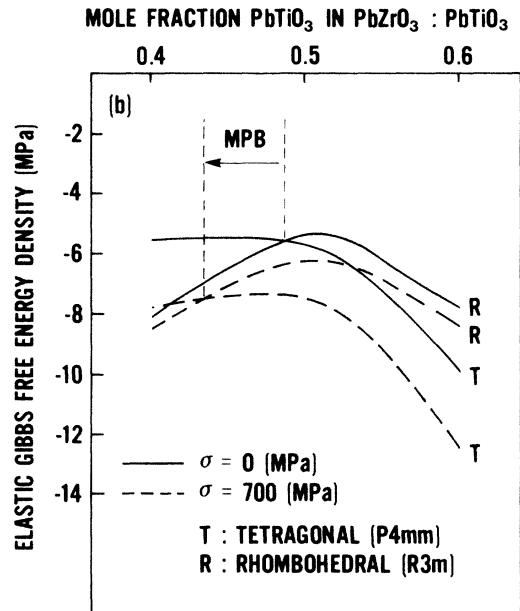
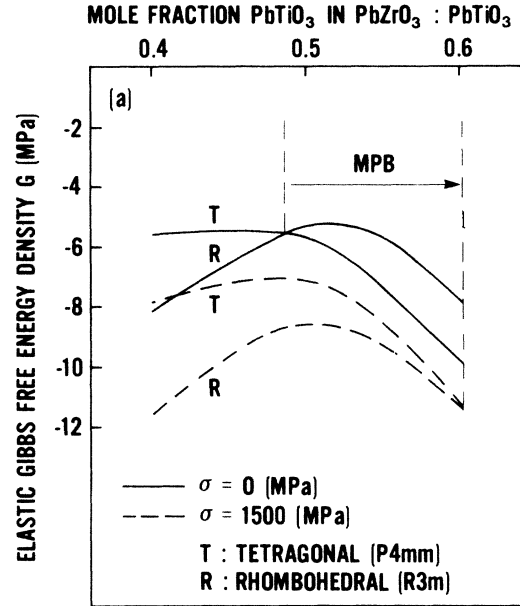


FIG. 2. Elastic Gibbs free energy under high hydrostatic pressure at 25° C for compositions close to the morphotropic phase boundary in the PbZrO_3 - PbTiO_3 system. (a) Tension. (b) Compression.

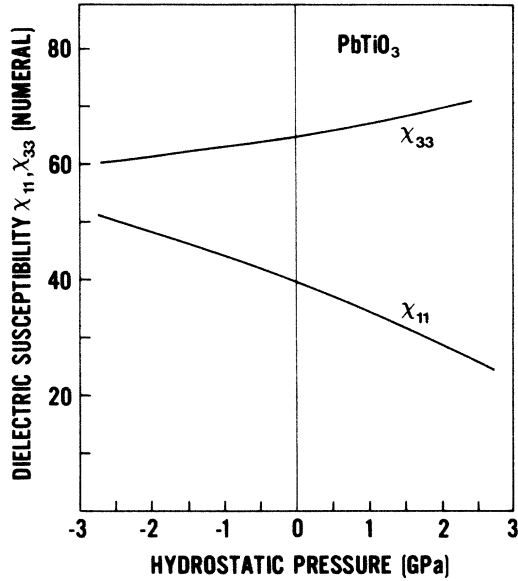


FIG. 3. Dielectric susceptibility at 25 °C as a function of hydrostatic pressure for single-domain—single-crystal PbTiO₃.

The first partial derivative equations give the electric field components,

$$\frac{\partial G}{\partial P_i} = E_i \quad (i = 1, 2, 3) . \tag{3}$$

The single-domain dielectric reciprocal susceptibilities (dielectric stiffnesses) are given by the second partial derivatives of the free energy function,

$$\frac{\partial^2 G}{\partial P_i \partial P_j} = 1/\chi_{ij} \quad (i, j = 1, 2, 3) \tag{4}$$

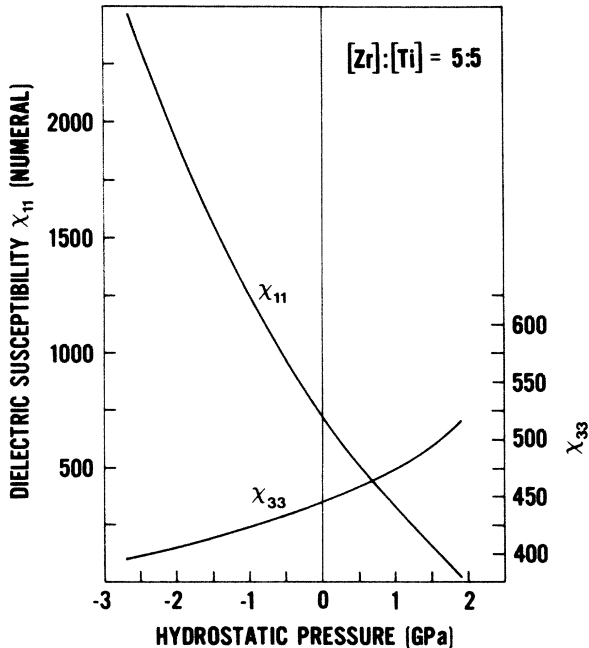


FIG. 4. Dielectric susceptibility at 25 °C as a function of hydrostatic pressure for single-domain—single-crystal Pb(Zr_{0.5}Ti_{0.5})O₃.

TABLE I. Calculated values of T_c , Θ , $P_s(T_c)$, ϕ , and the α stiffness coefficients.

	Mole fraction PbTiO ₃ in PbZrO ₃ :PbTiO ₃										
	0	0.1	0.2	0.3	0.4	0.5	0.6	0.7	0.8	0.9	1
T_c (°C)	211.8	257.7	298.4	334.4	366.1	394.1	418.7	440.3	459.5	476.7	492.2
Θ (°C)	208.2	254.1	294.4	330.0	361.3	388.9	413.1	433.9	451.5	465.6	475.9
$P_s(T_c)$ (C/m ²)	0.119	0.140	0.161	0.183	0.207	0.231	0.256	0.282	0.309	0.336	0.365
α_{11}^X (10 ⁵ m/F) at T_c	13.55	13.45	13.07	8.650	4.695	3.814	5.519	12.43	26.37	41.45	61.38
α_{11}^X (10 ⁷ m/F) at 25 °C	-6.894	-8.533	-8.857	-5.938	-3.289	-2.669	-3.795	-7.963	-14.02	-16.41	-16.97
α_{11}^X (10 ⁷ m ² /C ² F)	-19.10	-13.70	-10.07	-5.153	-2.226	-1.431	-1.677	-3.139	-5.535	-7.294	-9.235
ϕ	9.80	7.62	5.44	3.26	1.08	-1.10	-3.28	-5.46	-7.64	-9.82	-12.0
α_{12}^X (10 ⁷ m ² /C ² F)	-187.2	-104.4	-54.78	-16.80	-2.404	1.574	5.500	17.14	42.28	71.63	110.8
α_{11}^X (10 ⁸ m ³ /C ⁴ F)	67.33	35.16	19.41	7.658	2.605	1.342	1.279	1.974	2.903	3.223	3.469
α_{12}^X (10 ⁹ m ³ /C ⁴ F)	6.021	5.960	5.260	3.116	1.565	1.173	1.565	3.116	5.260	5.960	6.021
α_{123}^X (10 ⁹ m ³ /C ⁴ F)	-33.87	-31.66	-26.30	-14.60	-6.846	-4.767	-5.868	-10.71	-16.44	-16.76	-15.05

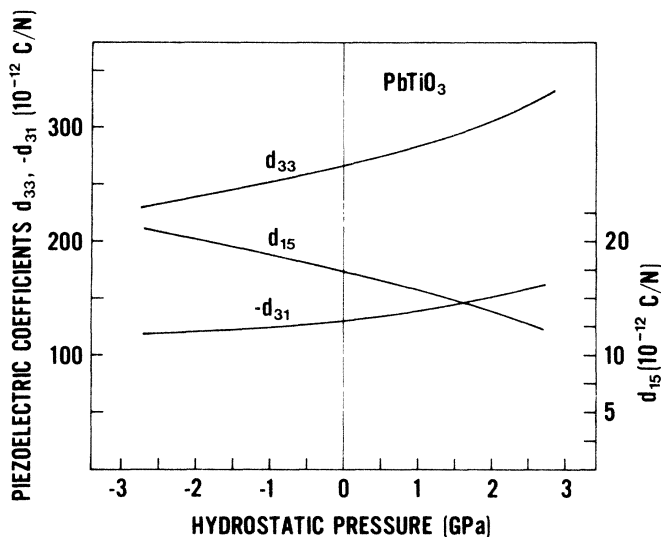


FIG. 5. Piezoelectric d_{ij} coefficients as a function of hydrostatic pressure for single-domain PbTiO_3 .

The piezoelectric coefficients are obtained from the following relation

$$d_{mkl} = (\epsilon_0) \chi_{mj} Q_{ijkl} P_i, \quad (5)$$

where ϵ_0 is the free-space permittivity (8.854×10^{-12} F/m).

Choosing an appropriate value for σ (hydrostatic pressure), the first derivative equations $\partial G / \partial P_i = E_i = 0$ ($i = 1, 2, 3$) are solved to give new values of polarization P_i under stress, which can then be reinserted in Eq. (2) to delineate G as a function of composition, temperature, and applied stress. A FORTRAN code was written to carry out the computation on an IBM 360 mainframe computer. In the computational procedure, the following values were used for electrostriction and elastic compliance coefficients:^{4,8} $Q_{11} = 0.065 \text{ m}^4/\text{C}^2$, $Q_{12} = -0.032 \text{ m}^4/\text{C}^2$, $s_{11}^P = 6.785 \times 10^{-12} \text{ m}^2/\text{N}$, and $s_{12}^P = -2.5 \times 10^{-12} \text{ m}^2/\text{N}$.

For compositions near the morphotropic phase boundary, the resulting free energies at 0 and 1500 MPa hydrostatic tension are shown in Fig. 2(a) and for 0 and 700 MPa hydrostatic compression in Fig. 2(b). The orthorhombic state is found to be metastable at all pressure levels for all single-cell compositions. Therefore, the orthorhombic free energies have been omitted from both figures for clarity. The hydrostatic pressure dependence of the single-domain—single-crystal dielectric susceptibility tensor at 25°C is computed from Eq. (4) and displayed in Fig. 3 for PbTiO_3 , and Fig. 4 for $\text{Pb}(\text{Zr}_{0.5}\text{Ti}_{0.5})\text{O}_3$. The piezoelectric moduli, as calculated from Eq. (5) as a func-

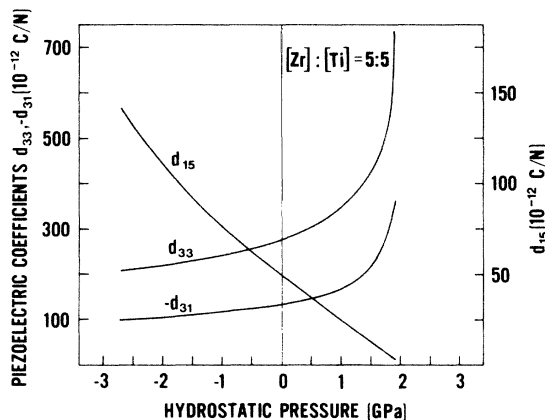


FIG. 6. Piezoelectric d_{ij} coefficients as a function of hydrostatic pressure for single-domain $\text{Pb}(\text{Zr}_{0.5}\text{Ti}_{0.5})\text{O}_3$.

tion of hydrostatic pressure, are depicted in Figs. 5 and 6 for PbTiO_3 and $\text{Pb}(\text{Zr}_{0.5}\text{Ti}_{0.5})\text{O}_3$, respectively.

DISCUSSION

The phenomenological analysis of the effect of hydrostatic pressure on the phase stability of morphotropic PZT compositions shows some expected results. The rhombohedral-tetragonal phase boundary is rather sensitive to changes in the elastic boundary conditions. A rhombohedral ($R3m$)—tetragonal ($P4mm$) phase transition can be induced in the morphotropic PZT compositions by the application of a relatively small hydrostatic pressure. This is not a surprising conclusion, since most of the lead-containing perovskites are known to have low elastic stiffness coefficients, and therefore are elastically soft materials. The Gibbs free-energy difference between stable and metastable phases at the PbTiO_3 composition agrees well with that proposed by Henning and Hardtl⁹ on empirical grounds, though from our calculations the free energies themselves are not a linear function of composition. It is interesting to note that at zero stress the dielectric anisotropy of the morphotropic PZT composition is opposite in sign to that of pure PbTiO_3 . In a future study, we intend to carry out an x-ray study using the opposed diamond-anvil—high-pressure cell to examine the morphotropic PZT composition under high hydrostatic pressure conditions to determine the morphotropic phase boundary shifts as a function of pressure.

¹B. Jaffe, W. R. Cook, Jr., and H. Jaffe, *Piezoelectric Ceramics* (Academic, New York, 1971).

²V. Ginzburg, *J. Exp. Theor. Phys. SSSR* **15**, 739 (1945).

³A. F. Devonshire, *Philos. Mag.* **40**, 1040 (1949).

⁴A. Amin, M. Haun, B. Badger, Jr., H. A. McKinstry, and L. E. Cross, *Ferroelectrics* **65**, 107 (1985).

⁵A. Amin, L. E. Cross, and R. E. Newnham, *Ferroelectrics* **37**, 647 (1981).

⁶A. Amin and L. E. Cross, *Jpn. J. Appl. Phys.* (to be published).

⁷G. R. Barsch, B. N. N. Achar, and L. E. Cross, *Ferroelectrics* **35**, 187 (1981).

⁸H. Landolt and B. Börnstein, *Ferroelectric and Antiferroelectric Substances* (Springer-Verlag, Berlin, 1975).

⁹D. Henning and H. K. Hardtl, *Proceedings of the International Conference on the Sciences of Ceramics* (Baden, West Germany, 1971) (unpublished).